Bulletin of the Seismological Society of America, Vol. 98, No. 4, pp. 1975–1982, August 2008, doi: 10.1785/0120070182

An M_L Scale in Northeastern Iran

by Jafar Shoja-Taheri, Saeid Naserieh, and Amir Hosein Ghafoorian-Nasab

Abstract Local-magnitude scales are derived for northeastern Iran (Khorasan province) from waveform data recorded at six stations from 205 local earthquakes, ranging in distance from 10 to 600 km. By averaging the horizontal components in a single measure, we used 1506 zero-to-peak amplitudes from synthetic Wood–Anderson seismograms to determine, in a least-squares sense, the appropriate $-\log A_0$ attenuation functions, the event local magnitude, and the station corrections. Both a parametric and a nonparametric description of $-\log A_0$ is considered while performing the inversions. In both cases, the constraint of 1-mm motion recorded at 100 km for M 3.0 earthquakes was used. To evaluate the distance correction curves in determining the local magnitude, M_L, in northeastern Iran we applied both linear and trilinear inversions to our datasets. The result of the linear inversion for distance correction is given by: $-\log A_0 = (1.370 \pm 0.050)\log(R/100) + (0.0020 \pm 0.0001)(R - 100) + 3$. For trilinear inversion we have applied the Monte Carlo technique. The resulting coefficients evaluated for the area are $R_1 = 106 \pm 5$ km; $R_2 = 347 \pm 49$ km; $n_1 = 1.380 \pm 0.045$; $n_2 = 0.597 \pm 0.132$; $n_3 = 0.415 \pm 0.236$; $k = 0.0033 \pm 0.0003$, where n_1, n_2, and n_3 are the coefficients of geometrical spreading for distances from the source to R_1, R_1 to R_2, and beyond R_2. k is the coefficient of inelastic attenuation. The remarkable agreement between the parametric and nonparametric results confirms that both linear and trilinear attenuation functions that we made for deriving the parametric distance correction are equally reasonable. Moreover, inversion of bootstrap replications of our dataset furnished stable solutions. Station magnitude corrections range between −0.17 and 0.27, suggesting a variable and noticeable effect of station-site properties on recorded amplitudes.

Introduction

The Khorasan province in northeastern Iran (the area under study) extends from 30° to 40° north latitude and from 52° to 62° east longitude (Fig. 1). The major tectonic provinces of the region are the Kopeh Dogh folded belt (Tchalenko, 1975), the eastern Alborz, and the central and eastern Iran province, an area of complex block movement. Near its southwest corner, the region approaches the Zagros main thrust line. Along its eastern edge, the region is bound by the north-south trending Harirud fault that, despite its current aseismic character and pre-Jurassic age (Stöcklin, 1974), serves as a boundary between the aseismic zone of western Afghanistan and the highly seismic region of northeastern Iran (Shoja-Taheri and Niazi, 1981). The Khorasan province, as a region with a high level of seismic activity, has suffered numerous destructive earthquakes throughout its long history, including four major ones in 1968, 1978, 1979, and 1997.

Local magnitude, M_L, was the first magnitude scale to describe the size of an earthquake. It was first developed by Richter (1935) for earthquakes in southern California. The local magnitude is based on the amplitude recorded by the Wood–Anderson torsion seismograph with a natural period of 0.8 sec, a damping constant of $h = 0.8$, and a static magnification of $V = 2800$. After Uhrhammer and Collins (1990), the magnification value has been recalibrated to 2080. However, because the value of 2080 has not been accepted as standard yet, in the present study we prefer to adopt 2800 in order to produce local magnitudes comparable with those predicted by scales calibrated before 1990. For local and regional distances, the M_L scale provides the best consistency and stability, so it is now widely used. But the large variability of velocity and attenuation structure of the Earth's crust does not, in fact, permit to develop a unique, internationally standardized calibration function for local events. Therefore, to secure consistency of the M_L scale, it is necessary to calibrate it for any region. A calibrated earthquake catalog based on M_L is of great importance for seismic hazard studies. Moreover, the value of the correction for amplitude decrease with distance gives useful insight for a better understanding of seismic-wave propagation in the area. In

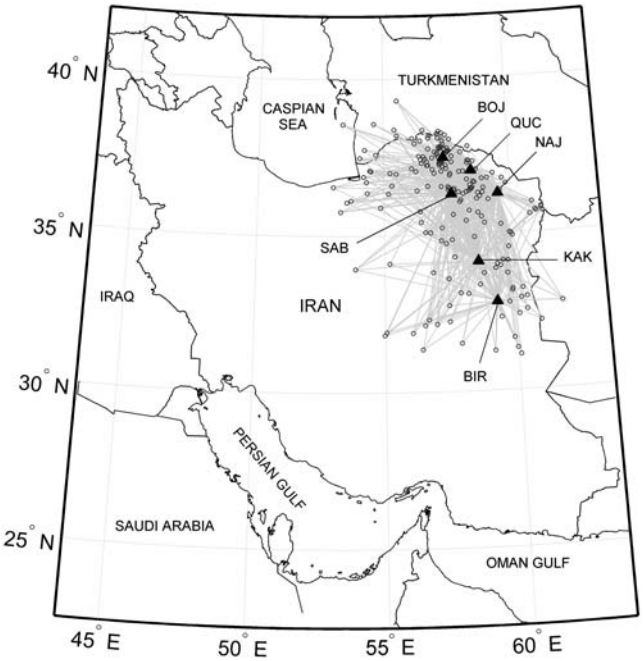

Figure 1. The station location (triangle and station identification) and the path (thin gray line) from the epicenter (open circle) to station.

this article, we calibrate M_L for northeastern Iran using synthetic Wood–Anderson seismograms (Kanamori and Jennings, 1978) calculated from the broadband data that have been recorded by the Khorasan Seismic Network (http://seismo.um.ac.ir, KHSN in the following) between 2002 and 2006. We follow both the Richter (1958) and Hutton and Boore (1987) approaches. The reliability of the results is validated by means of bootstrap analysis (Efron, 1979).

There have been several studies of attenuation in Iran. Nuttli (1980) has shown that for 1-sec period P_g, S_n, and L_g waves, the coefficient of anelastic attenuation has an average value of 0.0045 km^{-1}, similar to that for California but much greater than that for eastern North America. Chandra *et al.* (1979) pointed out that the average attenuation of intensities in Iran is slightly more rapid than the San Andreas province attenuation. Using L_g/P_g ratios, Al-Damegh (2004) inferred that the attenuation in the seismically active region of the eastern part of the Iranian Plateau is, expectedly, larger than that in the stable Arabian shield. Shoja-Taheri (2002) derived attenuation relations for peak and response spectra of the strong-motion data for different parts of Iran, including for eastern Iran. In a recent study Shoja-Taheri *et al.* (2007) developed relations for M_L scales in the main tectonic regions of the Iranian plateau using strong-motion data recorded within 250 km of epicentral distances. In their study, they performed the hinged trilinear form of attenuation (see Atkinson and Mereu, 1992) to avoid the negative values of k, the anelastic parameter, which were derived from a linear regression analysis. Using the strong ground-motion data from the 26 December 2003 Bam, Iran, earthquake, Shoja-Taheri and Ghofrani (2007) have recently evaluated the frequency-dependent intrinsic attenuation factors of $Q(f) = 352f^{1.02}$ in the frequency range of 0.3–10 Hz.

In this study, we evaluate the stability of our results by following two approaches to characterize the amplitude decay with distance. The first approach is to adopt parametric forms for linear (e.g., Hutton and Boore, 1987) and trilinear attenuation decays (e.g., Atkinson and Mereu, 1992; Shoja-Taheri *et al.*, 2007) and to compare the results of these inversions. The second approach is to seek a nonparametric and smooth description of decay with distance, in order to check the validity of the parametric models, without adopting any assumed parametric form (e.g., Richter, 1935; Cleveland and Devlin, 1988). Moreover, we use bootstrap analysis with 3000 inversions of the resampled dataset to estimate the uncertainties of the attenuation functions and station corrections.

Data

We used waveforms recorded by three-component, high-dynamic-range seismometers. The data come from six permanent stations of the KHSN equipped with Guralp CMG-3T (flat response between 0.01 and 50 Hz) velocimeters, connected through dial-up lines to the acquisition center. Data acquisition was performed at a sampling rate of either 25 or 125 samples per second; the waveforms of those events with magnitudes smaller than 3.5 are among the records that have been digitized with the rate of 125 samples per second. Figure 1 shows the KHSN stations and also reports the recorded seismicity used in this study to calibrate the local-magnitude scale for northeastern Iran (NEI). The data used in this study comprise 753 two-component horizontal velocity time series recorded for 205 earthquakes that occurred between 2002 and 2006 with magnitudes between 1.5 and 6.0. We have selected only those earthquakes that are registered by at least three stations within 600 km of epicentral distances. The six stations are listed in Table 1, where we also report the number of recordings from each station and the main characteristics of the stations (code, location, site geology, station corrections, and working period). The distance versus magnitude distribution of the recordings is shown in Figure 2. It is desirable to work with datasets with a lowest possible correlation between magnitude and distance (Joyner and Boore, 1981; Dahle *et al.*, 1990; Alsaker *et al.*, 1991). The data shown in Figure 2 have a weak correlation coefficient between magnitude and distance of 0.45.

Local-Magnitude Scale

Local magnitude was defined by Richter (1935, 1958) as:

$$M_L = \log A - \log A_0 + S, \tag{1}$$

Table 1
Stations Used in the Present Study

Code	Number of Records	Station Correction		Location			Site Geology	Working Period (mm/yyyy)
		Inversion	Bootstrap's Results	Latitude (°N)	Longitude (°E)	Elevation (m)		
BOJ	256	−0.097	−0.096 ± 0.016	37.482	57.386	1233	Limestone	Since 05/2002
QUC	328	0.269	0.269 ± 0.013	37.039	58.476	1547	Pyroclastic sediments	Since 03/2001
NAJ	352	−0.170	−0.170 ± 0.013	36.282	59.503	1206	Metamorphic Rocks	Since 04/2000
SAB	194	−0.105	−0.104 ± 0.016	36.306	57.683	1289	Igneous Rocks	Since 02/2004
KAK	258	−0.052	−0.052 ± 0.014	34.138	58.634	1861	Dark Shale	Since 08/2000
BIR	118	0.155	0.155 ± 0.020	32.835	59.288	1598	Alluvium	Since 08/2000

where A is the observed maximum amplitude of the horizontal Wood–Anderson seismometer recordings, A_0 is a distance-dependent attenuation curve, and S is a station-dependent M_L adjustment. The value of $-\log(A_0)$ is usually constrained at a reference R_{ref}. The Richter reference earthquake produces an amplitude of 1 mm on a Wood–Anderson seismograph located 100 km from the epicenter. A reference local magnitude, $V_{ref} = 3$, is given to this earthquake. The reference distance can be different from 100 km, and obviously, V_{ref} has to be changed accordingly. For instance, as suggested by Jennings and Kanamori (1983), using $R_{ref} =$ 10 km would be more likely to give a magnitude representative of source characteristics, and Hutton and Boore (1987) recommended $R_{ref} = 17$ km when a near-source anchoring is required. In any case, as pointed out by Alsaker *et al.* (1991) and Spallarossa *et al.* (2002), the attenuation function has to be evaluated with sufficient precision down to the assumed reference distance; that is, the analyzed seismicity must well sample the hypocentral distance shorter than R_{ref}. To ensure that this condition is fulfilled, the preferred reference distance is the one that allows, in the distance range of interest, a sufficient anchoring to a reference magnitude scale (Spallarossa *et al.*, 2002). According to the magnitude-distance distribution shown in Figure 2, we preferred

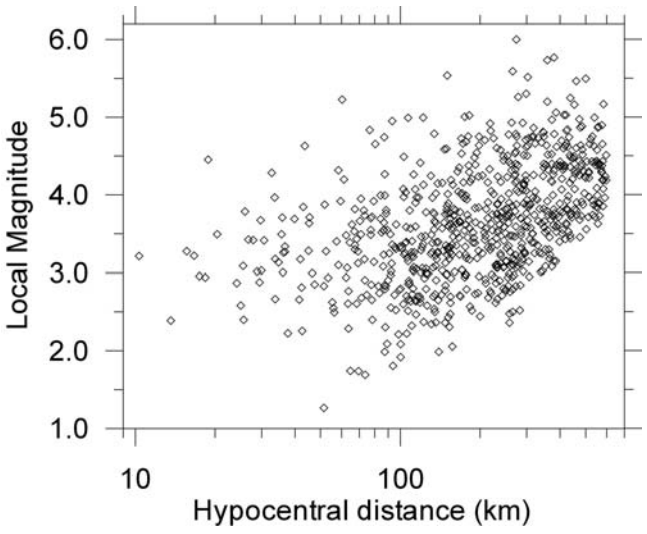

Figure 2. Distribution of the magnitudes of the selected earthquakes versus distance.

$R_{ref} = 100$ km in determining the attenuation curve using linear inversion.

Parametric Inversions

For parametric linear inversion, we refer to the model adopted by Bakun and Joyner (1984):

$$-\log A_0 = n\log(R/100) + k(R-100) + 3.0, \quad (2)$$

where R is the hypocentral distance (in kilometers), and n and k are parameters related to the geometrical spreading and anelastic attenuation in the region. To establish the new local magnitude, we refer to the model used by Bakun and Joyner (1984) and combine equations (1) and (2) to give:

$$\log A_{jl} = -n\log\frac{R_{jl}}{100} - k(R_{jl}-100) + \sum_{i=1}^{ne} M_i\delta_{ij} + \sum_{k=1}^{ns} S_k\delta_{kl} - 3.0, \quad (3)$$

where A_{jl} is the maximum zero-to-peak amplitude of earthquake j at the l station; R_{jl} is the hypocentral distance for earthquake j at station l; M_j is the local magnitude of the j earthquake; δ_{ik} and δ_{lj} are the Kronecker delta that allow the use of dummy variables; S_k is the corresponding station correction; ne and ns are the number of events and stations, respectively. The parameters to be determined regressively are n, k, S_k, and M_j representing, respectively, the geometrical spreading, anelastic attenuation, and station adjustment and magnitude, under the constraint that the station corrections sum to zero ($\sum S_k = 0$).

Following Spallarossa *et al.* (2002), the inversion of the linear system in equation (3) is performed by applying a least-squares procedure based on the LSQR algorithm (Paige and Saunders, 1982). We use the bootstrap technique (e.g., Efron, 1979; Efron and Tibshirani, 1993) to estimate the inversion stability; station corrections, attenuation parameters, and magnitude values are calculated by averaging the results of 3000 repeated inversions on randomly resampled datasets. Bootstrap results are also used to estimate the standard deviation of the parameters.

The constraint on station correction affects the M_L scale because a trade-off exists between magnitude and station cor-

rection. Because detailed information about most of the recording sites were not available, we set the average correction for the network equal to zero. The result of regression obtained by applying the LSQR procedure leads to $n = 1.377$, $k = 0.0019$ km^{-1}. Figure 3 shows the distance-dependence curve obtained by applying the LSQR procedure. To validate the reliability of the parameters retrieved from the LSQR technique, we compare them with the bootstrap results. In the lower panels of Figure 3, the distributions of the n and k values as derived by the bootstrap procedure are reported. These parameters appear normally distributed, with mean values of $n = 1.370 \pm 0.050$ and $k = 0.0020 \pm 0.00013$ km^{-1} similar to the values obtained from non-bootstrap inversion. The uncertainties are standard errors. Although the minimum root-mean-square error occurs at $n = 1.370$, there is a trade-off between n and k, and the minimum is broad. The parametric linear inversion leads to the following attenuation function:

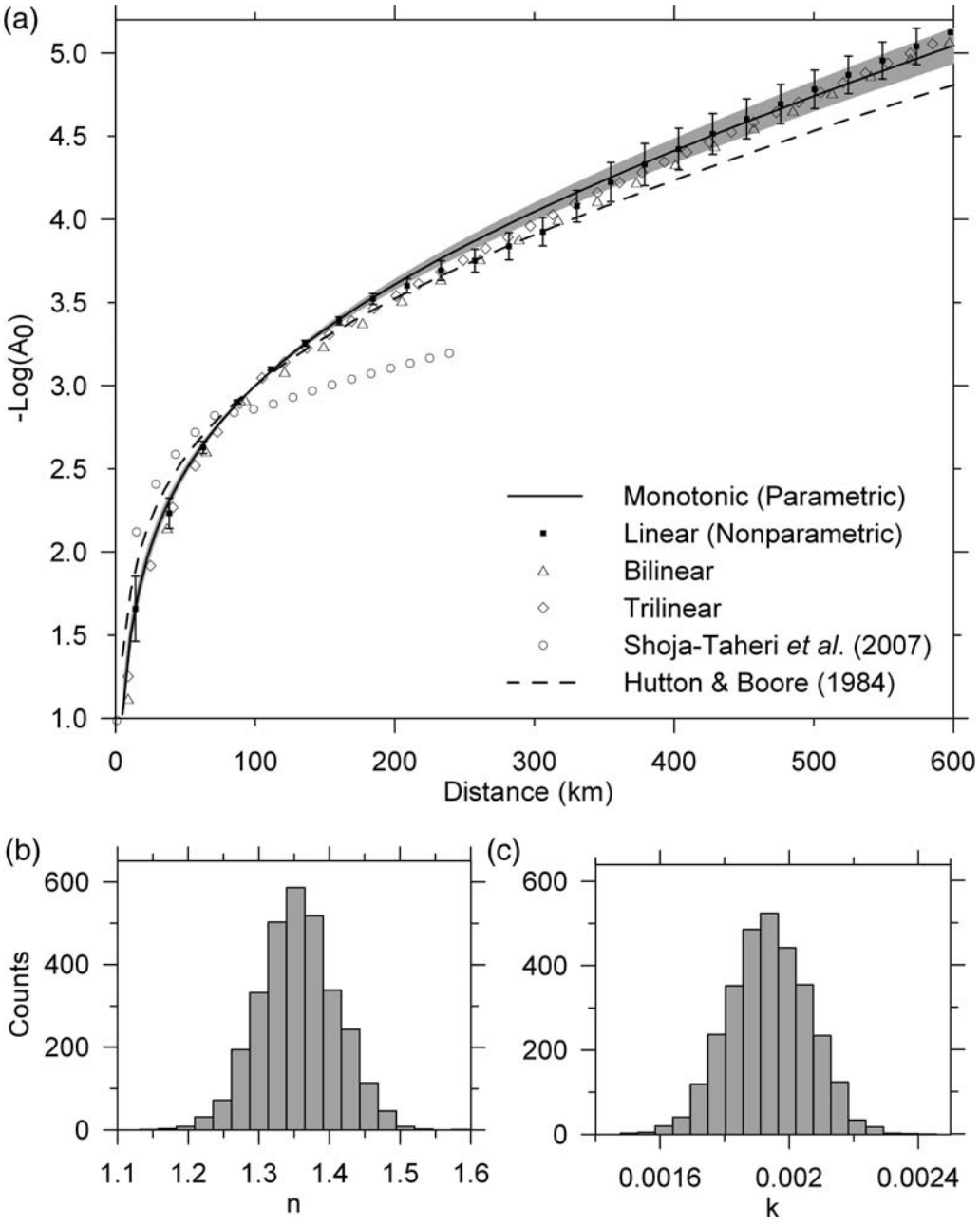

Figure 3. (a) A_0 curves from the present study for parametric (thick line), nonparametric (squares), and trilinear (diamonds) inversions, along with the Shoja-Taheri *et al.* (2007) attenuation function for eastern Iran (circles) and Hutton and Boore (1987) attenuation function for southern California (dashed line). Gray shaded area and vertical bars are mean ± 1 standard deviations for parametric and nonparametric results, respectively, as derived by inversions. Distribution for (b) n and (c) k parameters obtained performing 3000 bootstrap inversions.

$$-\log A_0 = (1.370 \pm 0.050)\log(R/100) + (0.0020 \pm 0.0001)(R - 100) + 3. \quad (4)$$

The result of the linear regression has shown that the value of n (and k) is strongly dependent on the selected distance range. Its value decreases with increasing the lower side and increases with lowering the upper limit of the distance range (for example, we obtained $n = 1.171$ for $R =$ 30–600 km and $n = 1.675$ for $R =$ 0–400 km). Therefore, validity of the assumption of a simple shape for the attenuation curve, with a constant geometrical spreading, n, along a broad range that includes both near-source and regional distances, seems to be questionable. The wave propagation studies indicate that the expected shape of amplitude decay for simple layered crustal models is complex (e.g., Burger *et al.*, 1987; Ou and Herrmann, 1990; Atkinson and Mereu, 1992). Layering in the crust causes direct-wave amplitudes to decay more steeply than R^{-1}. Then, as the direct arrivals are joined by postcritical reflection off the Moho and intracrustal discontinuities, there may be distance ranges where amplitudes actually increase with distance. Atkinson and Mereu (1992) have shown that the attenuation curve in southeastern Canada has three distinct sections.

Following Shoja-Taheri *et al.* (2007) a trilinear inversion is also performed allowing n to take different values along different segments of the distance range. To estimate the coefficients of the attenuation function, we employed the Monte Carlo technique (see Shoja-Taheri *et al.*, 2007 for more details) by generating random numbers confined within the predefined ranges for each of these parameters, testing all possible combinations of the attenuation parameters, and searching for the combination that minimizes the average residual errors under the constraints $-\log A_0(100) = 3$ and $\sum S_k = 0$. The inversion was performed using the LSQR method. The predefined windows for the parameters and their corresponding values evaluated for the region are given in Table 2. The trilinear shape of attenuation is shown in Figure 3.

Nonparametric Inversion

Nonparametric inversion is commonly introduced when the parametric model is unknown or must be checked. To check the results of the parametric models, we followed the method of locally weighted smoothing scatter plots introduced by Cleveland and Devlin (1988) by choosing the smoothing parameter as 0.7 and the fitting degree as 2. The inversion was performed using the LSQR method under the constraints of $-\log A_0(100) = 3$ and adopting the station corrections evaluated by the parametric inversions. The standard deviations for nonparametric results are derived by performing 3000 bootstrap inversions. The nonparametric decay curve is shown in Figure 3.

The parameter k can be related to the anelastic attenuation coefficient Q. However, it should be noted that because of the trade-offs between n and k, any inference for Q that is tied to the related value of n may be questionable. The Q/f ratio is calculated according to the formula given by Bakun and Joyner (1984),

$$Q/f = \pi/(V_s k \ln 10). \quad (5)$$

The average S-wave crustal velocity $V_s = 3.5$ km/sec is assumed. Q (1 Hz) values corresponding to k values of 0.002 and 0.003, which are obtained from the linear and trilinear inversions, are about 200 and 130, respectively. These low-Q values for the northeastern Iran agree with the results given by Nuttli (1980). He showed that the attenuation of 1-sec period crustal phases in Iran is relatively high with an apparent Q of 200 for L_g, 150 for S_n, and 125 for P_g. Xie (1993) obtained L_g coda $Q(1\text{ Hz}) = 200$–250 for Iran and Sarker and Abers (1998) obtained $Q_S = 309f^{0.30}$ and $Q_c = 195f^{0.65}$ for Kopet Dagh in the north of Khorasan province. Using the strong ground-motion data from the 26 December 2003 Bam, Iran, earthquake, Shoja-Taheri and Ghofrani (2007) have recently evaluated the frequency-dependent intrinsic attenuation factors of $Q(f) = 352f^{1.02}$ in the frequency range of 0.3–10 Hz.

Station Correction

The values of station adjustments and their corresponding standard deviations achieved by both nonbootstrap and bootstrap inversions are listed in Table 1. Both inversions give similar values of adjustments for each station. Figure 4 shows the distribution of the station-correction results as derived by 3000 bootstrap inversions. The standard deviation σ of the distributions relevant to the stations varies between 0.015 and 0.033. σ increases when the number of recorded events decreases (see Table 1).

In general, corrections for stations located on sediments or weathered rocks are positive, whereas corrections for sta-

Table 2
Parameters of Trilinear Attenuation Function

R_1	R_2	n_1	n_2	n_3	k
Predefined windows of parameters					
100–300 km	250–400 km	0.5–1.6	−0.5–1.2	0.1–1.6	0.0010–0.0050
Results					
106 ± 5	347 ± 49	1.380 ± 0.045	0.597 ± 0.132	0.415 ± 0.236	0.0033 ± 0.0003

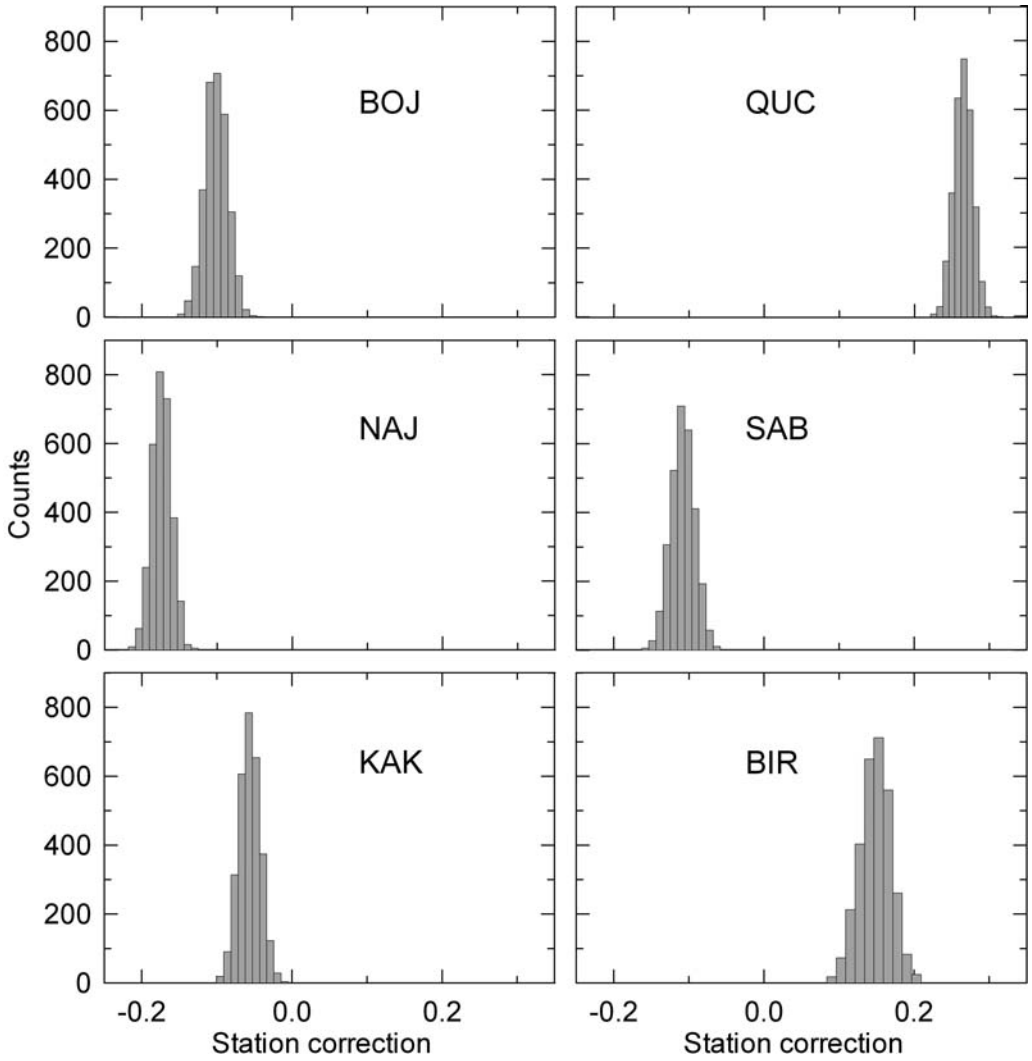

Figure 4. Magnitude station corrections: examples of distributions with respect to 3000 bootstrap replicates of the dataset used in the present study.

tions sited on hard rocks are near zero or negative. As shown in Figure 4, correction of stations BOJ, NAJ, KAK, and SAB, which are sited on rocks (see Table 1), are negative or near zero, whereas QUC and BIR stations, which are sited on sediment and alluvium, are positive.

Attenuation Functions

Figure 3 shows the distance-dependent curves obtained by applying both parametric and nonparametric approaches. The parametric approach includes linear and trilinear inversions. The nonparametric curve confirms that both linear and trilinear curves adequately and almost equally describe the attenuation in NEI. The differences between the mean values never exceed the value of 0.1. Moreover, the small standard deviation of the parametric bootstrap result (gray area) confirms the stability of the parametric linear inversion. The attenuation curves shown in Figure 3 imply weaker attenuation with respect to the relationship for southern California (Hutton and Boore, 1987) for distances shorter than 100 km and stronger attenuation for distances longer than 100 km. The attenuation curve for eastern Iran based on the recorded strong-motion data (Shoja-Taheri *et al.*, 2007) shows apparently drastic deviations from the curves derived in this study. It shows considerably weaker attenuation for distances longer than 100 km (about 0.5 units at 250 km) and stronger attenuation for distances shorter than 100 km. The differences between the shapes of these curves may be viewed as the result of employing different magnitude and distance ranges for the recorded strong-motion and the broadband datasets, because the group of phases that are dominant in shaping the attenuation curves may be different for different distance and magnitude ranges. We, therefore, believe that the attenuation functions derived from the broadband data (this study) and from the strong-motion data are both equally valid for determining the local magnitudes of the events in the area when using their related datasets.

Resulting Magnitude Relation

In Figure 5 the magnitude residuals (the difference between the average magnitude and the magnitude for each station) computed using the southern California curve (Fig. 5a) are compared with the residuals obtained by adopting the linear attenuation curve (equation 4) without any station correction (Fig. 5b) and with station correction (Fig. 5c). Figures 5d and 5e show the residuals using the trilinear attenuation function (Table 2) without and with station correction, respectively. The residuals do not show clear dependence on distance. The standard deviation is about 0.24 adopting southern California and is about 0.22 and 0.16 adopting NEI attenuation curves, respectively, before and after including the station correction. The results are similar for both linear and trilinear attenuation curves. The reduction of about 33% in standard deviation confirms that the attenuation and station corrections resulting from both linear and trilinear inversions lead to a better data fit and thus to reliable local-magnitude values.

Conclusions

The local-magnitude scales for NEI have been derived by analyzing 1506 readings from 205 earthquakes. Simulated Wood–Anderson seismograms were obtained by removing the instrument response and convolving for the standard Wood–Anderson torsion seismograph response. The linear and trilinear inversions lead to distance corrections given by equation (3) and by the parameters reported in Table 2.

A distance normalization of 1-mm motion recorded at 100 km for an M 3.0 earthquake was used. The linear and trilinear distance corrections both show lower attenuation with distance in NEI below 100 km and higher attenuation above the normalization distance, in comparison with

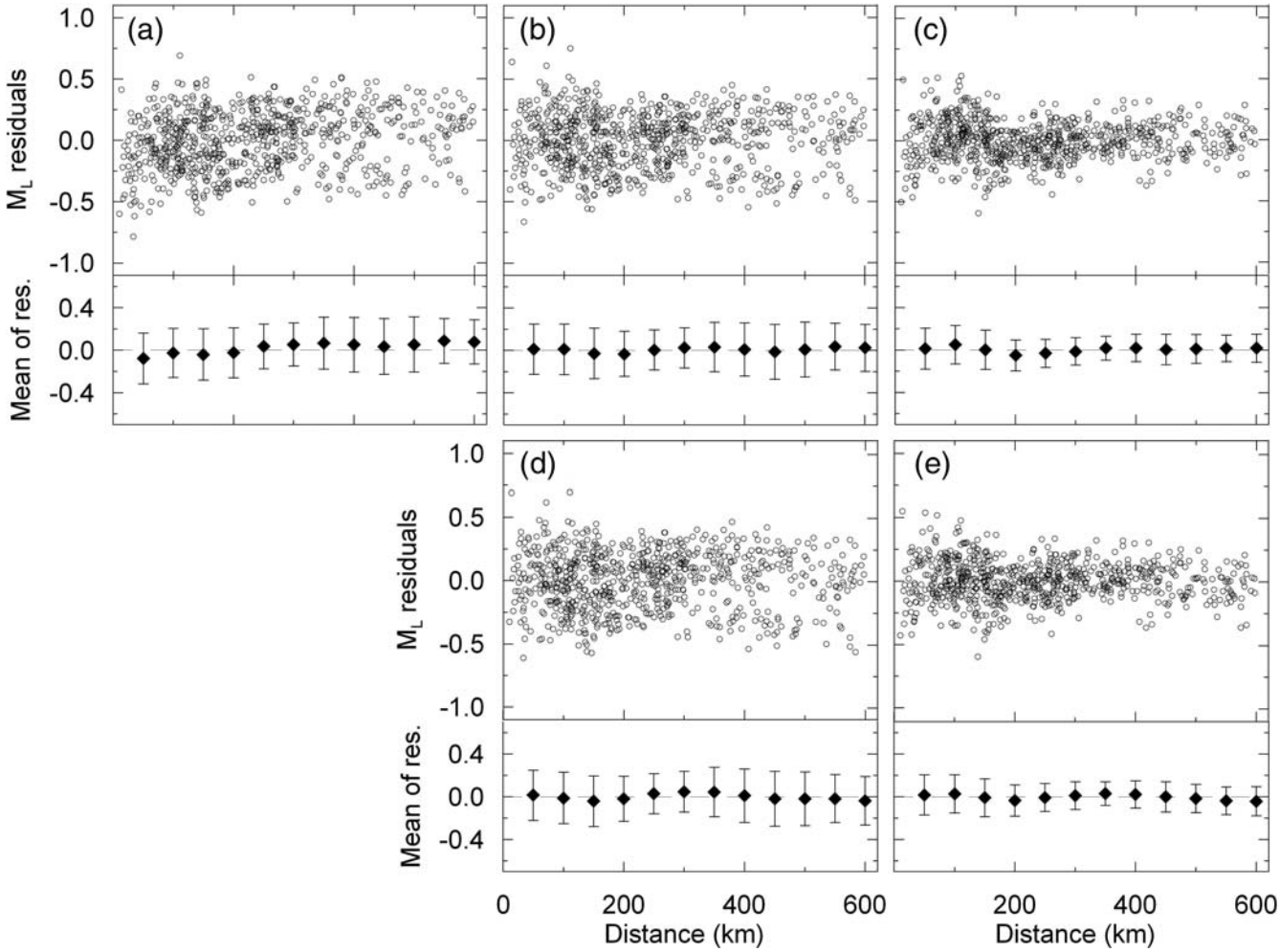

Figure 5. Local-magnitude residuals versus hypocentral distance. (a) The magnitudes are computed using Hutton and Boore (1987) attenuation coefficients without any station correction. (b) The magnitude residuals are computed using the attenuation function resulting from the linear inversion of the present study without any station correction and (c) with station correction. The magnitude residuals are computed using the attenuation function resulting from the trilinear inversion of the present study (d) without any station correction and (e) with station correction.

southern California. The remarkable agreement between the parametric (both linear and trilinear) and nonparameric distance corrections that we also computed confirms that the assumptions about the parametric distance corrections were reasonable. The inversion of 3000 bootstrap replications of our datasets indicated that the available data are adequate for a reliable and stable local-magnitude scale. Station magnitude corrections, based on linear and trilinear inversions, range between −0.16 and 0.27, suggesting a variable effect due to station-site properties.

Acknowledgments

We thank Associate Editor Gail Atkinson, Dino Bindi, and Simona Petrosino for their detailed and constructive reviews of the article. We also thank Hadi Ghofrani for his help in the preparation of the figures.

References

Al-Damegh, K., E. Sandovol, A. Al-Lazki, and M. Barzangi (2004). Regional seismic wave propagation (L_g and S_n) and P_n attenuation in the Arabian Plate and surrounding regions, *Geophys. J. Int.* **157,** 775–795.

Alsaker, A., L. B. Kvamme, R. A. Hansen, A. Dahle, and H. Bungum (1991). The M_L scale in Norway, *Bull. Seismol. Soc. Am.* **81,** 379–398.

Atkinson, G. M., and R. F. Mereu (1992). The shape of ground motion attenuation curves in southeastern Canada, *Bull. Seismol. Soc. Am.* **82,** 2014–2031.

Bakun, W. H., and W. B. Joyner (1984). The M_L scale in central California, *Bull. Seismol. Soc. Am.* **74,** 1827–1843.

Burger, R., P. Somerville, J. Barker, R. Herrmann, and D. Helmberger (1987). The effect of crustal structure on strong motion attenuation relations in eastern North America, *Bull. Seismol. Soc. Am.* **77,** 420–439.

Chandra, U., J. G. McWhorter, and A. A. Nowroozi (1979). Attenuation of intensities in Iran, *Bull. Seismol. Soc. Am.* **69,** 237–250.

Cleveland, W. S., and S. J. Devlin (1988). Locally weighted regression: an approach to regression analysis by local fitting, *J. Am. Stat. Assoc.* **83,** 596–610.

Dahle, A., H. Bungum, and L. B. Kvamme (1990). Attenuation models inferred from intraplate earthquake recordings, *J. Earthq. Eng. Struct. Dyn.* **19,** 1125–1141.

Efron, B. (1979). Bootstrap methods, another look at the jackknife, *Ann. Stat.* **7,** 1–26.

Efron, B., and R. J. Tibshirani (1993). *An Introduction to the Bootstrap*, Chapman and Hall, London.

Hutton, L. K., and D. M. Boore (1987). The M_L scale in southern California, *Bull. Seismol. Soc. Am.* **77,** 2074–2094.

Jennings, P. C., and H. Kanamori (1983). Effect of distance on local magnitude found from strong-motion records, *Bull. Seismol. Soc. Am.* **68,** 265–280.

Joyner, W. B., and D. M. Boore (1981). Peak horizontal acceleration and velocity from strong-motion records including records from the 1979 Imperial Valley, California, earthquake, *Bull. Seismol. Soc. Am.* **71,** 2011–2038.

Kanamori, H., and P. C. Jennings (1978). Determination of local magnitude, M_L, from strong-motion accelerograms, *Bull. Seismol. Soc. Am.* **68,** 471–485.

Nuttli, O. W. (1980). The excitation and attenuation of seismic crustal phases in Iran, *Bull. Seismol. Soc. Am.* **70,** 469–485.

Ou, G., and R. Herrmann (1990). A statistical model for peak ground motion from local to regional distances, *Bull. Seismol. Soc. Am.* **80,** 1397–1417.

Paige, C. C., and M. A. Saunders (1982). LSQR: an algorithm for spars linear equations and spars least squares, *ACM Trans. Math. Softw.* **8,** 43–71.

Richter, C. F. (1935). An instrumental earthquake magnitude scale, *Bull. Seismol. Soc. Am.* **25,** 1–31.

Richter, C. F. (1958). *Elementary Seismology*, W. H. Freeman and Company, New York, 578 pp.

Sarker, G., and G. A. Abers (1998). Comparison of seismic body wave and coda wave measures of Q, *Pure Appl. Geophys.* **153,** 665–683.

Shoja-Taheri, J. (2002). Attenuation relations for peak and response spectra of horizontal acceleration from strong-motion records for the main seismic zones of the Iranian plateau (abstract), *Seism. Res. Lett.* **73,** 242 (SSA Spring Meet. Suppl.).

Shoja-Taheri, J., and H. Ghograni (2007). Stochastic finite-fault modeling of strong ground motion from the 26 December 2003 Bam, Iran, earthquake, *Bull. Seismol. Soc. Am.* **97,** 1950–1959.

Shoja-Taheri, J., and M. Niazi (1981). Seismicity of the Iran plateau and bordering regions, *Bull. Seismol. Soc. Am.* **71,** 477–489.

Shoja-Taheri, J., S. Naserieh, and H. Ghograni (2007). M_L and M_W scales in the Iranian Plateau based on the strong-motion records, *Bull. Seismol. Soc. Am.* **97,** 661–669.

Spallarossa, D., D. Bindi, P. Augliera, and M. Cattaneo (2002). An M_L scale in northwestern Italy, *Bull. Seismol. Soc. Am.* **92,** 2205–2216.

Stöcklin, J. (1974). Possible ancient continental margins in Iran, *Geology of Continental Margins*, C. A. Burk and C. L. Drake (Editors), Springer-Verlag, New York.

Tchalenko, J. S. (1975). Seismicity and structure of Kopeh Dagh (Iran, U.S.S.R.), *Phil. Trans. R. Soc. London* **278,** (1275), 1–25.

Uhrhammer, R. A., and E. R. Collins (1990). Synthesis of Wood-Anderson seismogram from broadband digital records, *Bull. Seismol. Soc. Am.* **80,** 702–716.

Xie, J. (1993). Simultaneous inversion for source spectrum and path Q using Lg with application to three Semipalatinsk explosions, *Bull. Seismol. Soc. Am.* **83,** 1547–1562.

Earthquake Research Center
Ferdowsi University of Mashad
Mashad, Iran
jshoja@yahoo.com
saeid.naserieh@gmail.com
Aghafoorian@yahoo.com

Manuscript received 16 July 2007